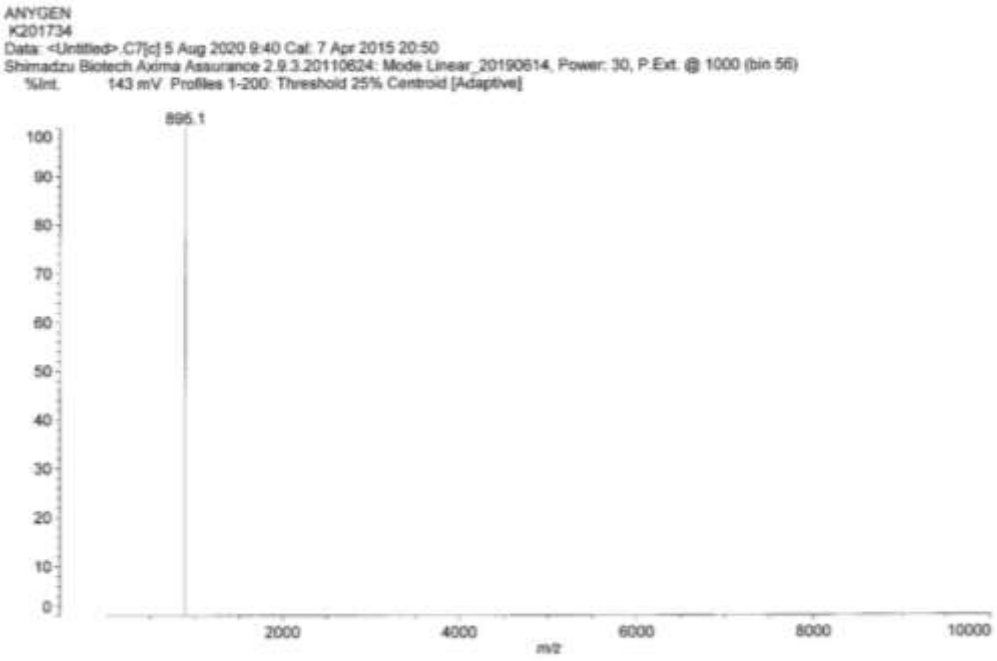

Supplemental Figure 1. Mass analysis of CRTpep. MS *m/z* expected $[M]^+$ = 895.1 Da; actual = 891.5 Da.

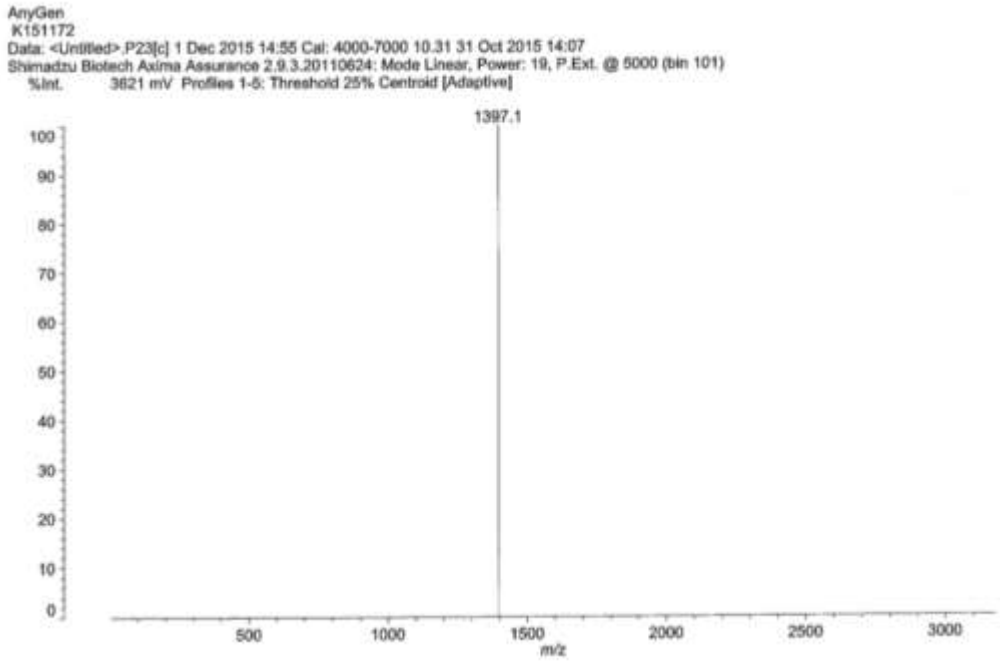

Supplemental Figure 2. Mass analysis of CRTpep-FITC. MS *m/z* expected $[M]^+$ = 1397.7 Da; actual = 1397.1 Da.

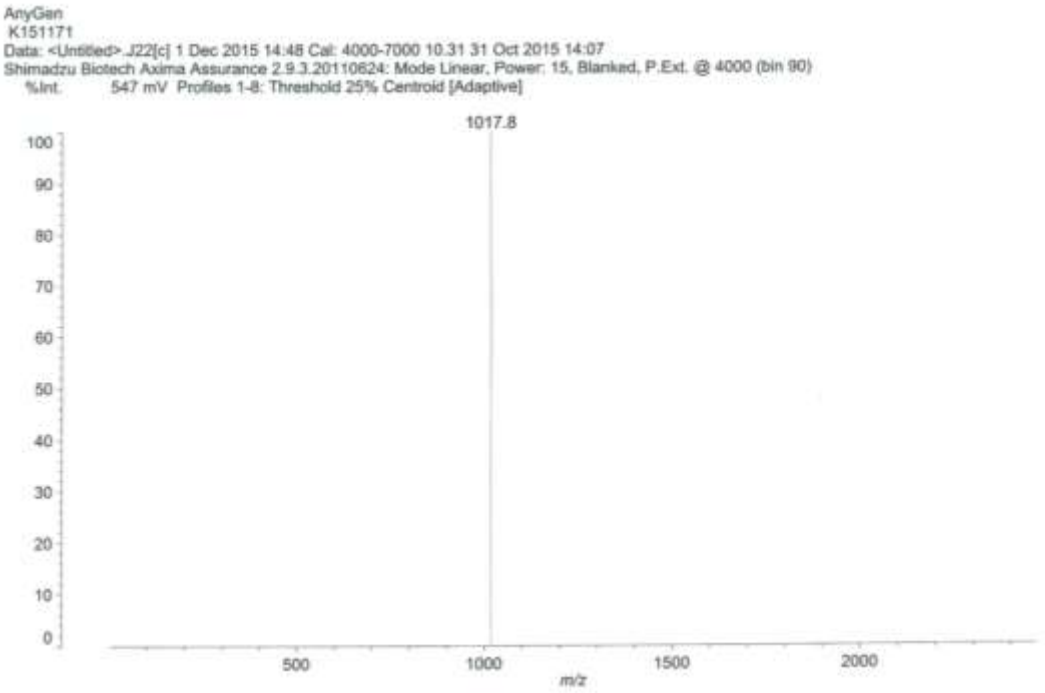

Supplemental Figure 3. Mass analysis of ^{19}F-CRTpep. MS *m/z* expected $[M]^+$ = 1018.2 Da; actual = 1017.8 Da.

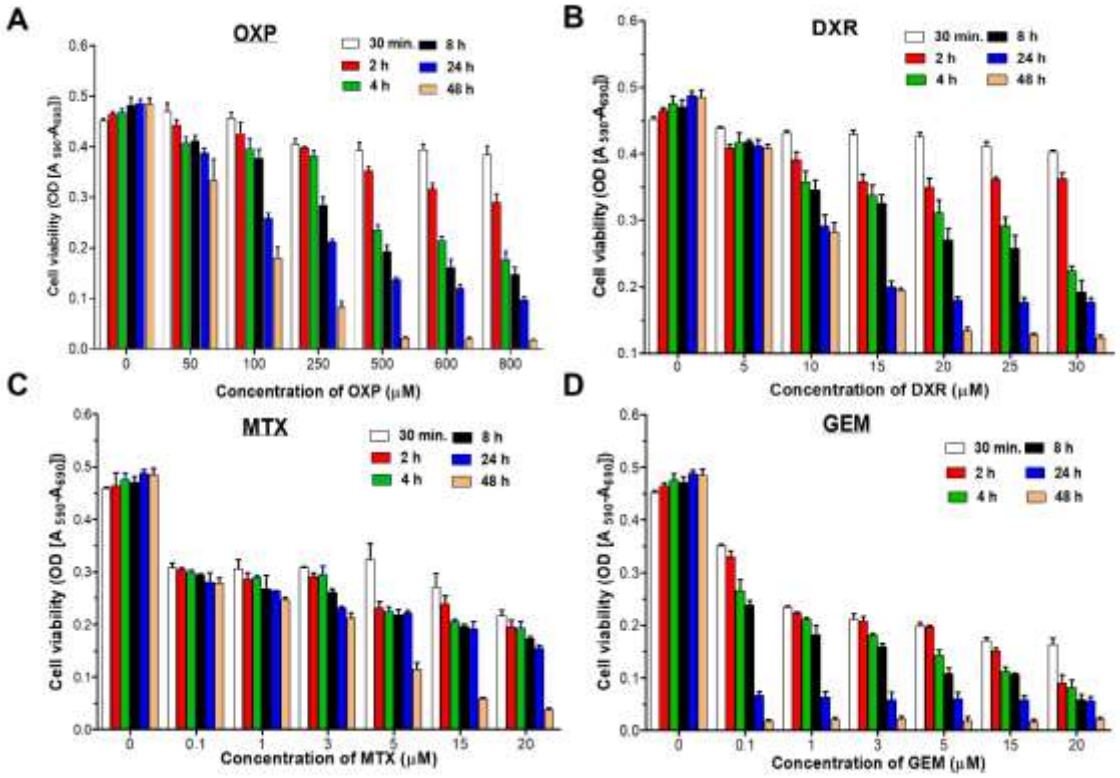

Supplemental Figure 4. Cytotoxicity of immunogenic and non-immunogenic drugs against CT26 cells. CT26 cells were cultured with immunogenic drugs (A) oxaliplatin (OXP), (B) doxorubicin (DXR), (C) mitoxantrone (MTX), and (D) the non-immunogenic drug gemcitabine (GEM) for the indicated times. Cell viability was measured using absorbance levels, the level of absorbance was calculated and expressed as the mean ± SD of three independent experiments.

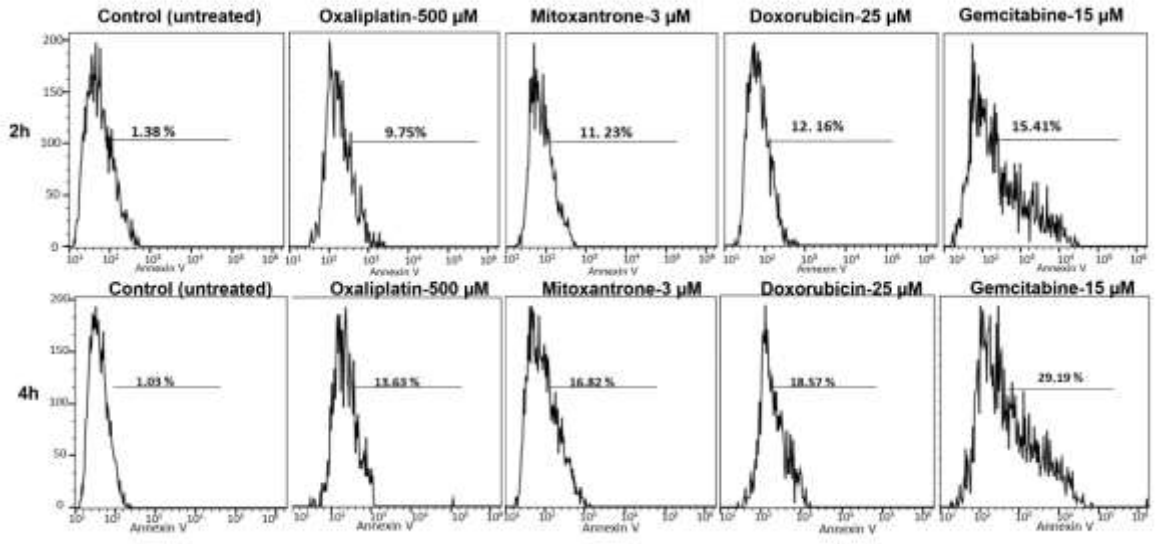

Supplemental Figure 5. Evaluation of apoptosis induced in CT26 cells by non-immunogenic and immunogenic drugs. Apoptotic death was assessed after treatment of CT26 cells with OXP (500 μM), DXR (25 μM), MTX (3 μM), or GEM (15 μM) for 2 and 4 h. Apoptotic induction was assessed using FITC-conjugated annexin-V and flow cytometry. The cell populations binding annexin-V (%) were gated and the percentage of apoptotic cells calculated.

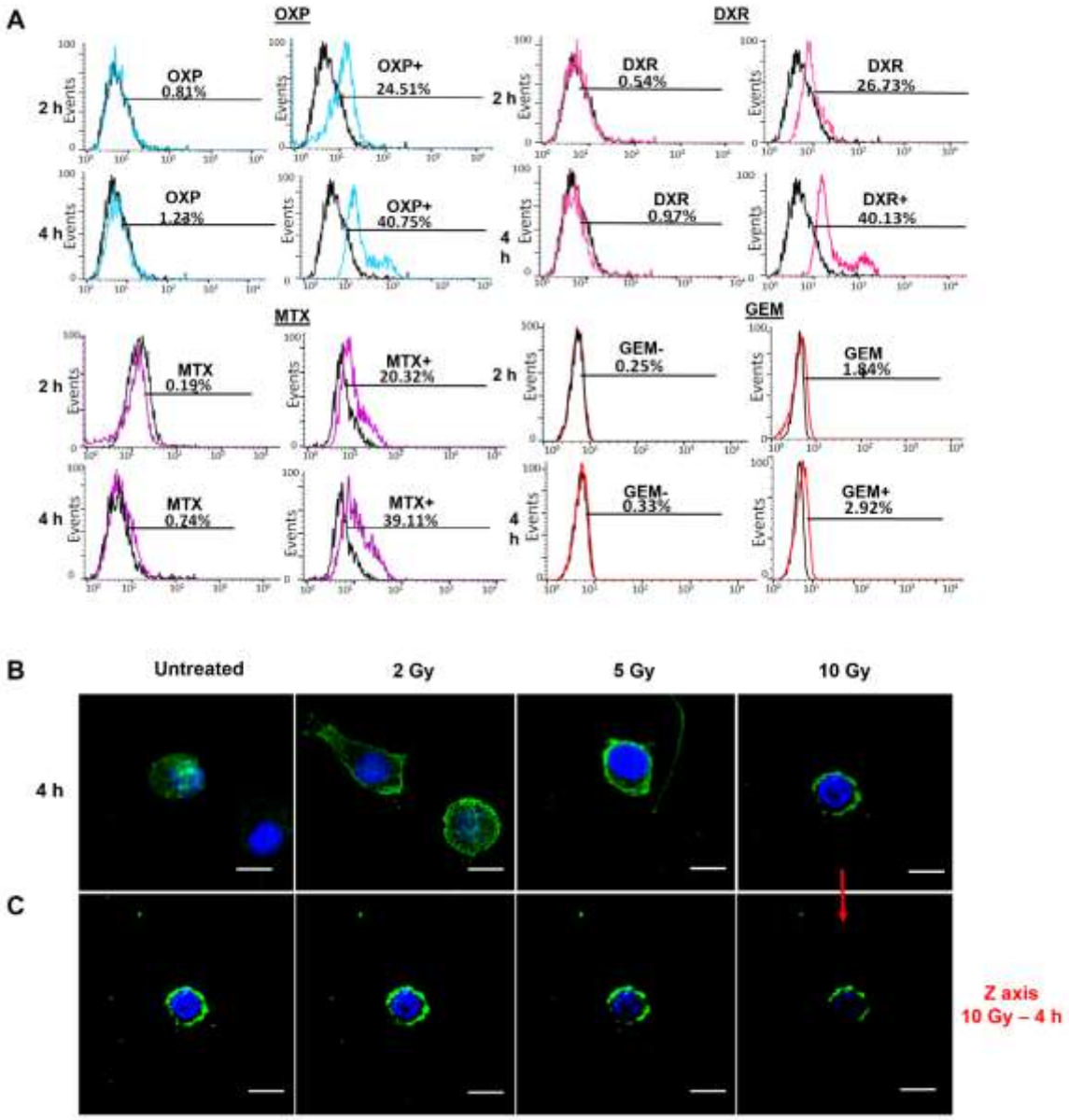

Supplemental Figure 6. (A) Analysis of translocated CRT by flow cytometry using a CRT-specific primary antibody. CT26 cells were treated with or without immunogenic (500 μM OXP, 25 μM DXR, 3 μM MTX) and non-immunogenic (15 μM GEM) drugs for 2 h or 4 h and then incubated with an anti-CRT antibody followed by an Alexa Fluor 488 secondary antibody to detect the ecto-CRT. The percentage of cells expressing ecto-CRT was calculated based on detected fluorescence levels (compared with the respective control group). (B) Confocal fluorescence microscopy analysis for CRT exposure in

irradiated CT26 cells. CT26 cells were irradiated at the indicated doses (2, 5, and 10 Gy) for 4 h and 24 h. The ecto-CRT was detected using an anti-CRT antibody (green) and nuclei were stained with DAPI (blue). Specific binding of CRT-antibody with ecto-CRT in CT26 cells after irradiation was observed using alexa fluor-488 labelled antibody under confocal laser scanning microscopy. Scale bar, 10 μm. (C) Representative confocal Z-slices are shown (arrow). Three-dimensional reconstruction sections are shown with fluorescence (Z section). Scale bar = 10 μm

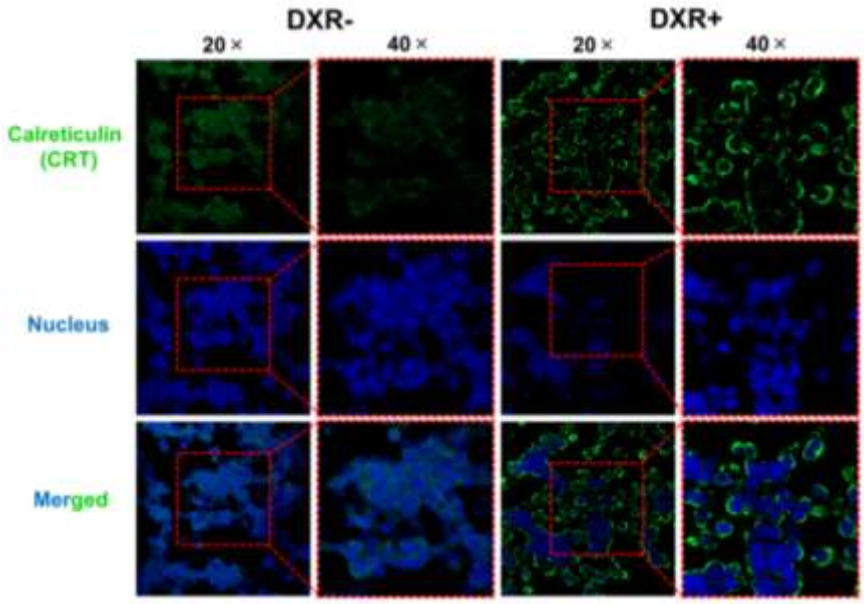

Supplemental Figure 7. Fluorescence microscopic analysis of *in vivo* expression of ectoCRT in immunogenically treated CT26 tumors. CT26 cells bearing tumor xenografts were treated with DXR (10 mg/kg) and the ectoCRT expression was detected using CRT specific antibody by confocal laser scanning microscopy (20 × and 40 × magnification). Image shows the, Green, CRT-antibody with Alexa 488 stained ectoCRT; blue and DAPI-stained nuclei.

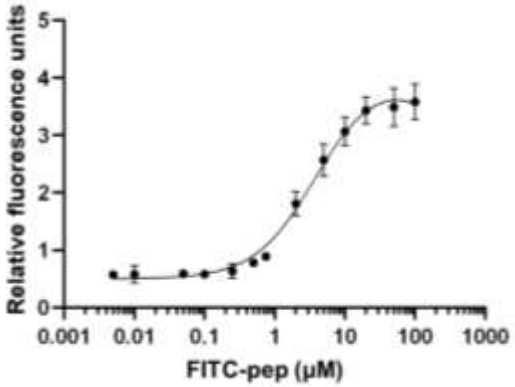

Supplemental Figure 8. Determination of the binding affinity of CRTpep to the recombinant CRT protein. Recombinant CRT (0.1 μg) were captured per well of 96 well ELISA plate and different concentration of FITC-CRTpep (100.0, 75.0, 50.0, 20.0, 10.0, 5.0, 2.0, 1.0, 0.75, 0.50, 0.25, 0.10, 0.05, 0.01, 0.005, 0.0 μM) were allowed to bound for 2 h at room temperature. Fluorescence intensity were measured and Kd value were calculated by nonlinear regression (curve fit) GraphPad Prism (K_d value of CRTpep= 1.868 μM).

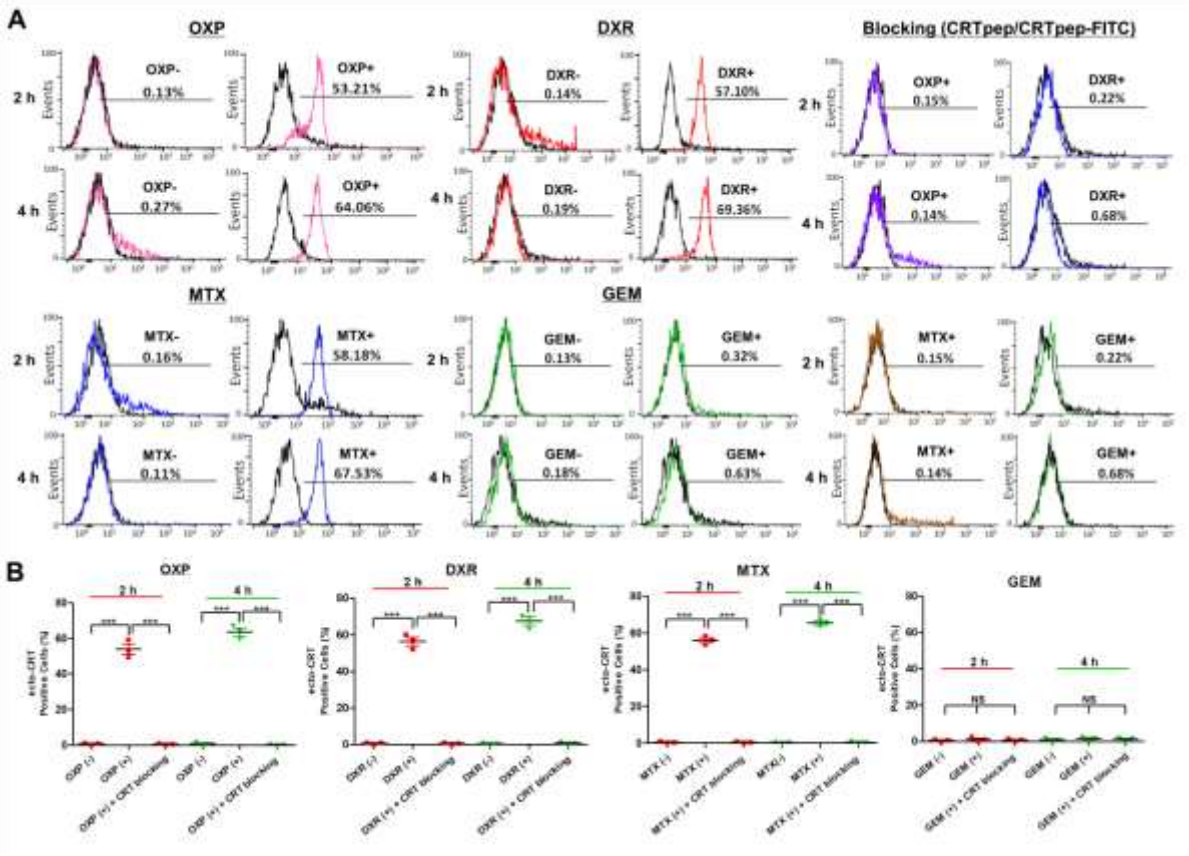

Supplemental Figure 9. Flow cytometry analysis of CRTpep binding to ecto-CRT after immunogenic and non-immunogenic drug treatment in B16F10 cells. (A) Flow cytometry analysis of CRTpep binding to ecto-CRT after immunogenic and non-immunogenic drug treatment in B16F10 cells. Binding of CRTpep-FITC to ecto-CRT in in B16F10 cells after 2 h and 4 h of anticancer drug (immunogenic and non-immunogenic) treatment was determined by flow cytometry. Percentage cellular uptake was calculated based on the detected mean fluorescence levels of untreated control cell. After anticancer drug treatment in B16F10 cells were pre-incubated with CRTpep (200 μM) for 1 h, followed by incubation with CRTpep-FITC (2 μM), and then was subjected to flow cytometry to detect uptake using fluorescence generated by the ecto-CRT. (B) Quantitative assessment of binding of CRTpep-FITC to ecto-CRT in in B16F10 cells after 2 h and 4 h of anticancer drug (immunogenic and non-immunogenic) treatment that was determined by flow cytometry. The data were analyzed with one-way ANOVA method and expressed as mean (± SD) fluorescence level. (n = 3; $^{***}P < 0.001$; ns = not significant).

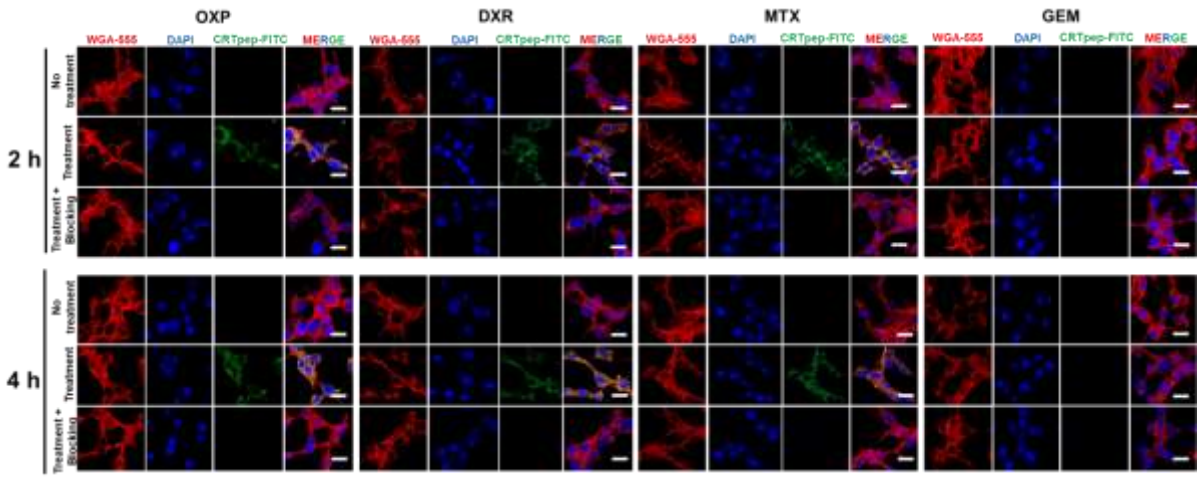

Supplemental Figure 10. Immunofluorescence staining and analysis of CRTpep binding to ecto-CRT after immunogenic and non-immunogenic drug treatment in B16F10 cells. Binding of CRTpep-FITC to ecto-CRT in B16F10 cells after 2 h and 4 h of anticancer drug (immunogenic and non-immunogenic) treatment was determined by confocal laser scanning microscopy (40 × magnification) after immunofluorescence staining. Green, CRTpep-FITC; blue, DAPI-stained nuclei; red, cell membrane stained with WGA-555. Scale bar, 50 μm. For the blocking assay, anticancer drug-treated cells were further incubated with 200 μM unlabeled CRTpep followed by 2 μM CRTpep-FITC. Scale bar, 50 μm.

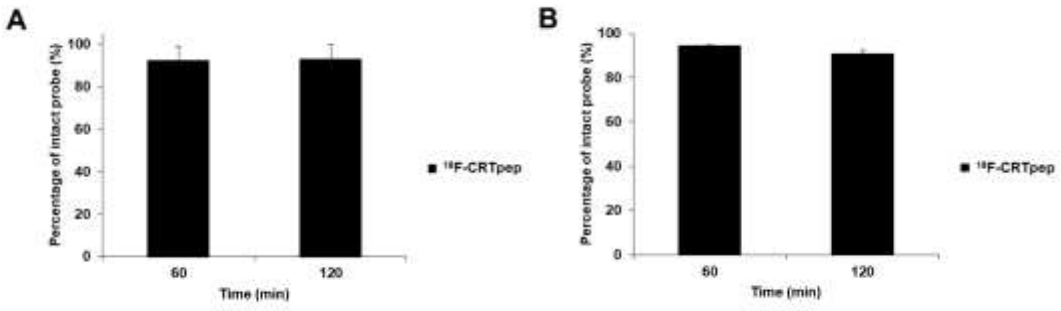

Supplemental Figure 11. Stability of ^{18}F-CRTpep. (A) *In vitro* stability of ^{18}F-CRTpep (0.74 MBq) in human serum at 60 min and 120 min after incubation (92.16 ± 6.80 at 60 min and 92.98 ± 7.16 at 120 min). (B) *In vivo* stability of ^{18}F-CRTpep (7.4 MBq/ 100 μL) at 60 min and 120 min incubation (94.30 ± 0.63 at 60 min and 90.62 ± 2.12 at 120 min). Stability was then analyzed by instant thin layer chromatography-silica-gel (iTLC-SG) developed with 0.1% TFA in D.W. and 0.1% TFA in acetonitrile (3 : 7) after 60 min and 120 min.

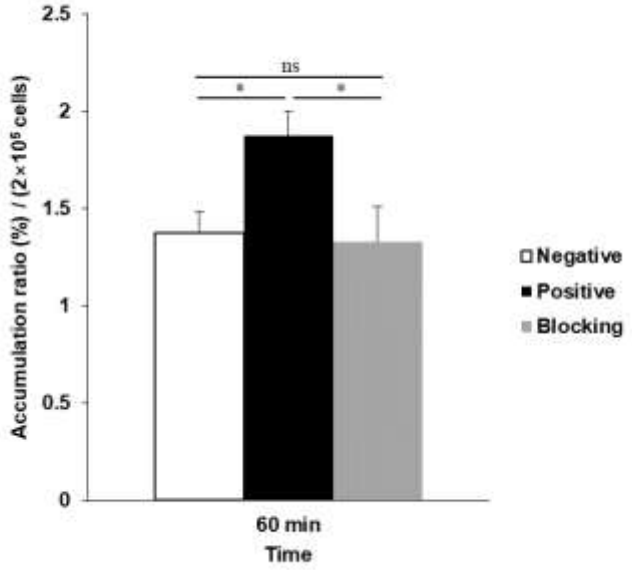

Supplemental Figure 12. *In vitro* cellular uptake of ^{18}F-CRTpep in CT26 after DXR treatment for 4 h. Blocking group was pretreated with CRT antibody (1 μg/ 0.5 mL) for 1 h. The cells were incubated with 0.74 MBq of ^{18}F-CRTpep for 60 min and washed twice with DPBS. The radioactivity of the supernatant and cell lysate was measured with a gamma counter. Data are expressed as the accumulation ratio (%) ± SD per 2 × 10^5 cells (Pyo et al. J Nucl Med 2018; 59:340–346). It was calculated by dividing the radioactivity in the pellet by the radioactivity in the supernatant and pellet combined. (Negative, Positive, Blocking group: 1.38 ± 0.11, 1.88 ± 0.12, 1.33 ± 0.18 at 60 min, **P* < 0.05; ns = not significant)

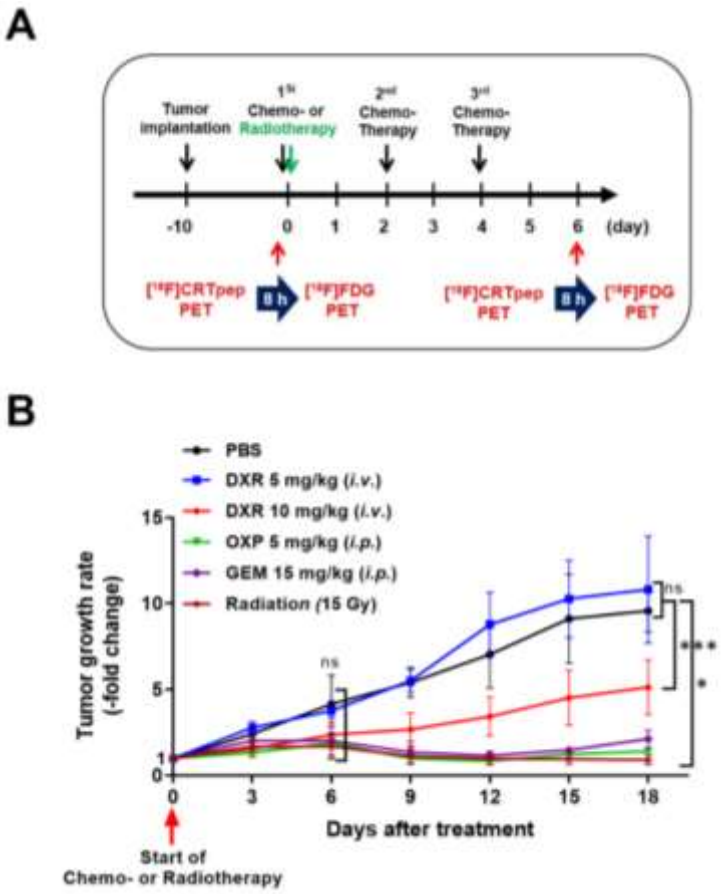

Supplemental Figure 13. Therapeutic effect of immunogenic and non-immunogenic drugs (DXR, OXP, GEM), and radiation in CT26-tumor bearing mice. (A) CT26- bearing mice were injected intravenously (*i.v*) or intraperitoneally (*i.p*) with DXR (5 mg/kg or 10 mg/kg), OXP (5 mg/kg), GEM (15 mg/kg), or PBS three times with a 2 day interval between each dose. Radiation (15 Gy) was given once. ^{18}F-CRTpep and ^{18}F-FDG animalPET were performed at 8-h intervals in the same animals. (B) Tumor growth rate was measured at indicated days after chemo- and radiation therapy (n = 6; $^{*}P < 0.05$; $^{***}P < 0.001$; NS = not significant; *P* value of PBS *vs* DXR (5 mg/kg), DXR (10 mg/kg), OXP, GEM, or radiotherapy on day 6: > 0.9999, = 0.6173, = 0.1416, = 0.195,5 or = 0.0804, respectively; *P* value of PBS *vs* DXR (5 mg/kg), DXR (10 mg/kg), GEM, or radiotherapy on day 18: > 0.9999, = 0.0006, = 0.0167, or = 0.0025, respectively).

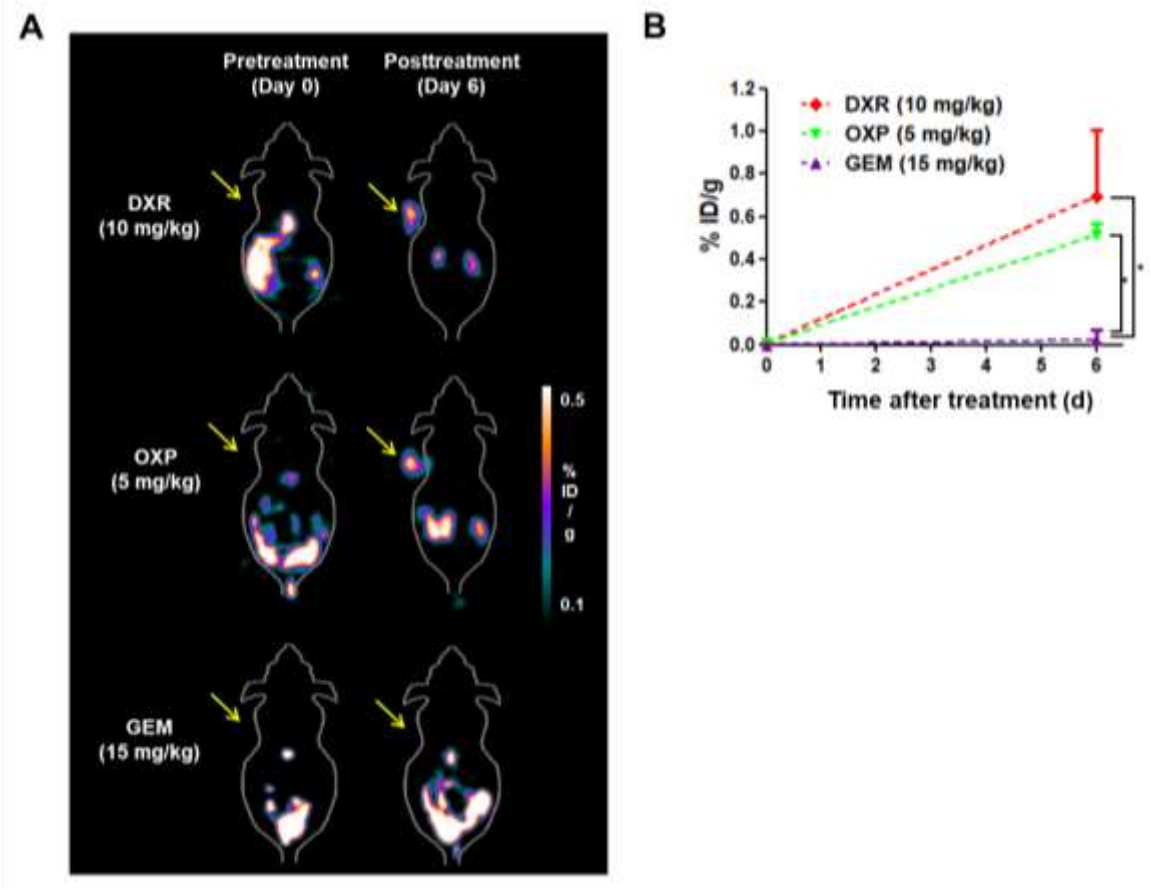

Supplemental Figure 14. Assessment of ICD by small animal PET using ^{18}F-CRTpep in B16F10 tumor-bearing mice. (A) Representative ^{18}F-CRTpep small animal PET images of B16F10-bearing mice. ^{18}F-CRTpep (7.4 MBq) was injected (*i.v.)* into mice before and at 6 days after chemotherapy. Arrows indicate subcutaneous tumors. (B) Quantification of ^{18}F-CRTpep small animal PET imaging signals in tumors before (day 0) and after treatment (DXR = 0.70 ± 0.31; OXP = 0.51 ± 0.06; GEM = 0.02 ± 0.04; **P* < 0.05).

Supplemental Table 1. Biodistribution of ^{18}F-CRTpep at 120 min after *i.v.* injection in CT26 tumor bearing mice 6 days after DXR treatment. Tumor, blood, and other organs were extracted and weighed, and the radioactivity in the organs was counted using a gamma counter. To obtain the %ID/g, radioactivity determinations were normalized against the weight of tissue and the amount of radioactivity injected (n = 4).

Organs	%ID/g
Blood	0.61 ± 0.36
Heart	0.20 ± 0.11
Lung	0.36 ± 0.24
Liver	0.35 ± 0.21
Spleen	0.31 ± 0.24
Stomach	0.17 ± 0.14
Intestine	2.22 ± 0.43
Kidney	4.61 ± 1.24
Pancreas	0.28 ± 0.19
Normal muscle	0.31 ± 0.17
Bone	0.31 ± 0.06
Skin	0.45 ± 0.29
Tumor	0.73 ± 0.34